

Ultrastructural changes during lung carcinogenesis-modulation by curcumin and quercetin

XIN WANG¹⁻³, LEI WANG¹, HAO ZHANG¹, KE LI¹ and JIQIN YOU¹

¹Department of Thoracic Surgery, Xuzhou Central Hospital, The Affiliated Xuzhou Hospital of Medical College of Southeast University; ²Department of Thoracic Surgery, Xuzhou Clinical School of Xuzhou Medical College; ³Department of Thoracic Surgery, Xuzhou Clinical Medical College of Nanjing University of Chinese Medicine, Xuzhou, Jiangsu 221009, P.R. China

Received April 20, 2016; Accepted July 28, 2016

DOI: 10.3892/ol.2016.5259

Abstract. The aim of the present study was to examine the effectiveness of curcumin and quercetin in modulating ultrastructural changes during lung carcinogenesis. A total of 24 male laka mice were divided into the normal control, benzo[*a*]pyrene (BP)-treated, BP+curcumin-treated, BP+quercetin- treated, and BP+curcumin+quercetin-treated groups (n=6 per group). Lung carcinogenesis was induced by a single intraperitoneal injection of BP [100 mg/kg of body weight (b.wt.)]. Curcumin was supplemented to mice at a dose level of 60 mg/kg of b.wt. in drinking water and quercetin was given at a dose level of 40 mg/kg of b.wt. in drinking water. The ultrastructure of BP-treated mice revealed disruptions in cellular integrity together with nuclear deformation and premature mitochondrial aging. Notably, supplementation with phytochemicals individually resulted in improvement of the ultra-histoarchitecture of BP-treated mice although the improvement was much greater with combined supplementation of phytochemicals. Furthermore, BP treatment revealed alterations in lung histoarchitecture, which, however, were improved appreciably following combined supplementation with curcumin and quercetin. The results of the present study show that, combined supplementation with curcumin and quercetin effectively preserved the histoarchitecture as well as ultra-histoarchitecture during BP-induced lung carcinogenesis in mice.

Introduction

Cancer is the second leading cause of mortality after heart disease (1). Cancer comprises a group of diseases characterized by the unregulated division and proliferation of cells. Lung

cancer is a leading causes of mortality in men and women (2). The main reason behind the discouraging survival statistics is that the majority of lung cancer subjects present with late-stage disease and are not curable using current therapies (3).

Chemoprevention is one of the promising areas in anticancer strategies in which extensive research is being performed globally. Use of the combination approach is an upcoming area of research (4). To the best of our knowledge, there is currently a paucity of information with regard to the combined use of curcumin and quercetin in modulating ultrastructural changes during lung cancer.

Thus, the focus of the present study was to evaluate the efficacy of the combined chemoprevention approach using curcumin and quercetin in modulating ultrastructural changes during lung carcinogenesis.

Materials and methods

Chemicals. Benzo(*a*)pyrene (BP), NADPH, GSH, NBT, DTNB, Curcumin and Quercetin was procured from Sigma-Aldrich (St. Louis, MO, USA).

Animals. A total of 24 male laka Mice, weighing 18-20 g, were procured from the Xuzhou Medical College (Jiangsu, China). The rats were housed in polypropylene cages in a temperature-controlled room (21±2°C) on a 12-h light/dark cycle (lights on at 06:00), and had free access to food and water. Prior to initiating the experiments, the animals were adapted to the laboratory conditions for a week. The study was approved by the Ethics Committee of Xuzhou Medical College.

Experimental design. The mice were divided into five treatment groups. Animals in group I served as normal controls and were given water and diet *ad libitum*. Mice in this group were also administered corn oil intraperitoneally, which was used as the vehicle for treatment in BP-treated animals. Animals in group II were given a single injection (P) of BP at a dose level of 100 mg/kg of body weight (b.wt.) dissolved in corn oil, for a total duration of 10 weeks (5). Group III animals were given curcumin at a dose level of 60 mg/kg of b.wt. three times a week orally in water. Animals in group IV were given quercetin at a dose level of 40 mg/kg of b.wt. in water three times a week

Correspondence to: Dr Lei Wang, Department of Thoracic Surgery, Xuzhou Central Hospital, The Affiliated Xuzhou Hospital of Medical College of Southeast University, 199 South Jiefang Road, Xuzhou, Jiangsu 221009, P.R. China
E-mail: ks227h@163.com

Key words: lung cancer, curcumin, quercetin, ultra structure

orally. Animals in group V animals were given a combined treatment of curcumin and quercetin in a similar manner as was given to group III and IV animals, respectively. The abovementioned treatment with phytochemicals was started 10 days prior to BP injection.

Ultrastructural studies. A small section of lung (1x1 cm; 4 μ m thick) was removed, immersed in PBS and fixed with formaldehyde and glutaraldehyde, prior to incubation in 0.2 M sodium cacodylate buffer (pH 7.2) for 10-12 h at 4°C. The specimens were then thoroughly washed 3 times in 0.1 M cacodylate buffer (Biosharp, Hefei, China) and post-fixed for 60 min in 1% osmium tetroxide (Biosharp), created in the cacodylate buffer. The tissues were thoroughly washed in buffer to remove any extraneous traces of osmium tetroxide and then dehydrated in ascending series of acetone, allowing 20 min per change, in each concentration of acetone. Specimens were then filtered and subsequently embedded in resin. Specimen blocks were formed by polymerization of the pure embedding resin at 60°C for 48-72 h. Ultrathin sections of various specimen blocks were made using ultramicrotome (Jiancheng Biotech, Nanjing, China). Initially, semithin sections (1 μ m) were cut using sharp glass knives to locate the area of interest in the different treatment groups. These semithin sections were stained with 0.5% toluidine blue produced in 1% borax solution. Ultrathin sections of interference colors from golden to silver were cut and loaded on fine copper grids. The sections were then double-stained with uranyl acetate and lead citrate. The ultrathin sections were subsequently reviewed under a transmission electron microscope (Olympus, Tokyo, Japan).

Results

Ultrastructure of lung of normal control mice. In the normal control group, the alveolar cells were normal in appearance with a normal nucleus with intact nuclear membrane (Fig. 1). Two types of alveolar cells are recognized, types I and II. The alveolar epithelium (type I) consisted of cells forming the thin layer of lining, with the alveolar air spaces with nucleus occasionally bulging into the alveolus lumen. Type II cells exhibited microvilli present on the surface of the alveolar epithelium of the mouse lung and seemed to be integral with neat arrangement. Mitochondria were many and they appeared to be regular in shape with approximate roundness and ellipse. The inner matrix of mitochondria was of medium density and the cell-to-cell contact was clearly distinct. Inclusion bodies were present in the type II cells. The type II cells contained remnants of surfactant-rich lamellar bodies. Surfactant released from these cells covered the alveolar surface to reduce surface tension in order that alveolar surfaces did not collapse onto one another on expiration. Multi-lobular nuclei were also observed. Additionally, vacuolization was observed once or twice in the normal control cells. The basement membrane was visible, forming an interface between alveolar and capillary endothelia. Red blood cells were also visible along with the nucleus of capillary cells.

Ultrastructure of lung of benzo[a]pyrene-treated mice. Changes in the ultrastructural appearance of lung cells (Figs. 2 and 3) were evident in carcinogenesis following

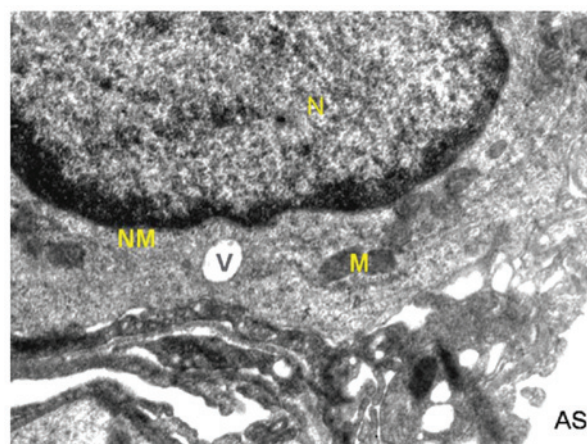


Figure 1. Ultrastructure of lung of normal control mice. The image shows an intact nucleus (N), nuclear membrane (NM), mitochondria (M), alveolar space (AS), vacuole (V) and intact capillary endothelium submerged with alveolar epithelium.

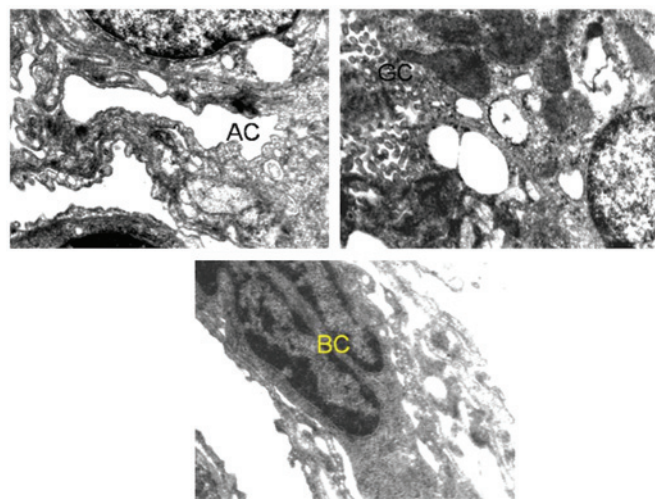


Figure 2. Ultrastructure of lung of benzo[a]pyrene-treated mice. The image shows alveolar constriction (AC), granular cytoplasm (GC), and bi-nucleated cells (BC).

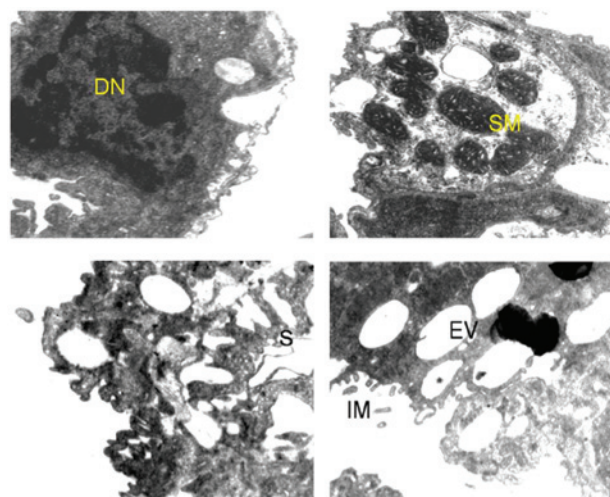


Figure 3. Ultrastructure of lung of benzo[a]pyrene-treated mice. The image shows disfigured nucleus (DN), swollen mitochondria (SM), space between capillary and alveolar epithelia (S), extensive vacuolization (EV), and irregular arrangement of microvilli (IM).

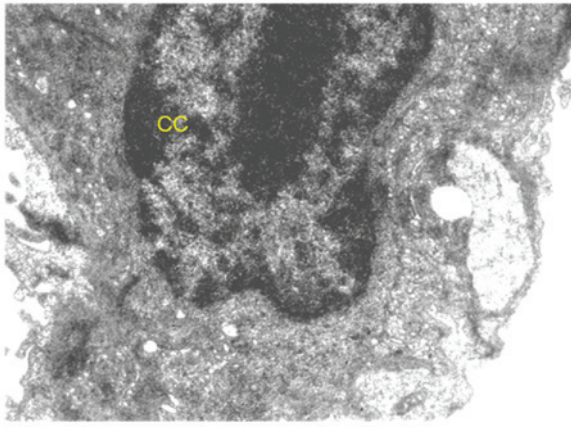


Figure 4. Ultrastructure of lung of benzo[a]pyrene+quercetin-treated mice. The image shows improved nuclear arrangement, and chromatin condensation (CC) decrease in vacuolization.

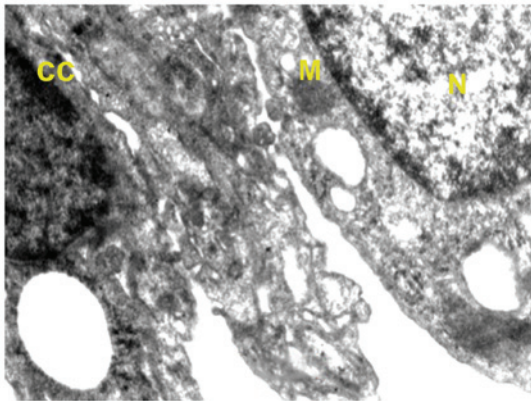


Figure 5 Ultrastructure of lung of benzo[a]pyrene+curcumin-treated mice. The image shows improved nuclear arrangement (N), chromatin condensation (CC), and normal size mitochondria (M).

benzo[a]pyrene treatment. The most obvious changes were seen in the shape of nucleus along with the disruption of nuclear envelope and lamina. Mitochondria were found to be swollen, elongated and with flocculent material, giving a denser appearance. The cytoplasm of cells was granulated and the vacuolization of inclusion bodies was also observed. Separation of endothelium and epithelium from the basement membrane of the alveolar was also observed.

Ultrastructure of lung of benzo[a]pyrene+quercetin-treated mice, benzo[a]pyrene+curcumin-treated mice, and benzo[a]pyrene+curcumin+quercetin-treated mice. Supplementation with curcumin (Fig. 4) and quercetin (Fig. 5) alone and in combination (Fig. 6) with benzo[a]pyrene-treated mice appreciably moderated the ultrastructural changes with regard to integrity of the cells as a whole as well as the cell organelles. However, chromatin condensation in nucleus and some vacuoles in the cytoplasm were evident.

Discussion

The results of the present study showed the synergistic potential of curcumin and quercetin in moderating alterations in

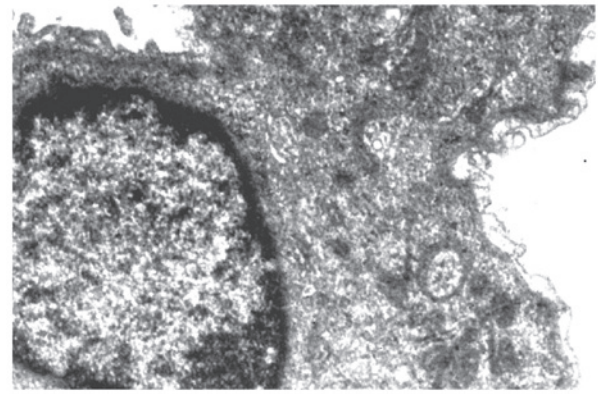


Figure 6. Ultrastructure of lung of benzo[a]pyrene+curcumin+quercetin-treated mice. The image shows improved nuclear arrangement, chromatin condensation (CC), normal mitochondria, and decrease in vacuolization.

ultra-structure in lung cells during experimentally-induced lung carcinogenesis in mice. Curcumin and quercetin collectively improved the majority of ultrastructural changes in lungs of BP-treated mice.

In the normal control mice, type I and II alveolar cells were recognized (6). The alveolar epithelium of type I consisted of cells forming a thin layer of lining of the alveolar air spaces with nuclei occasionally bulging into the alveolar lumen. Usually, the inter-alveolar septa is formed by alveolar epithelium of type I cells on either side of the lumen along with the capillary sandwiched between them and this arrangement was also visible in the ultrastructure of lung (7). The basement membrane of the three epithelia seems to be forged into one unit to form a continuous pattern of the inter-alveolar septa. This arrangement is necessary for the proper exchange of respiratory molecules of type II cells and for the presence of microvilli on the surface of the alveolar epithelium of the mouse lung (8).

Mitochondria were numerous in number and they appeared to have approximate roundness and be elliptical in shape. The inner matrix of mitochondria was of medium density and the cell-to-cell contact was clearly distinct. Additionally, inclusion bodies were present in the type II cells. Type II cells are responsible for the release of surfactant, which covers the alveolar surface to reduce surface tension in order that alveolar surfaces do not collapse onto one another on expiration. In the BP-treated group, the shapes of the nuclei were altered together with the disruption of nuclear envelope and lamina. This may be correlated with the formation of micronuclei as be evident in the micronucleus assay (9). Mitochondria were found to be swollen, elongated and filled with flocculent material, giving a denser appearance. The cytoplasm of cells were granulated and the vacuolization of the inclusion bodies was also observed. Separation of endothelium and epithelium from the basement membrane of the alveoli was also observed, which is indicative of injury (10). This result may well be correlated with the increase in the levels of tumor marker enzymes, especially lactate dehydrogenase (LDH), which is also a marker of tissue injury (11). The derangement of microvilli in the type II cells may be postulated to occur due to neoplastic changes occurring in the cells, which may be included the formation of intermediate forms of types I and II (12). In addition, there

may be a replacement of normal type II cells by the hyperplastic type II cells.

Supplementation with phytochemicals in individual and in combined form appreciably moderated the ultra-structural changes with regard to the integrity of the cells as a whole as well as the cell organelles. The presence of chromatin condensation observed in the nuclei is indicative of apoptosis, which is well substantiated by an increase in apoptotic cells (9). The nuclear envelope was intact, which may be correlated well with the decrease in the formation of micronuclei as observed by the micronucleus assay (13). A number of vacuoles decreased and the microvilli arrangement showed order signifying the protective role played by the phytochemicals. There was an improved arrangement of capillary endothelium with reduced separation of endothelium from the basement membrane of the alveoli that could well be linked with a decrease in the levels of LDH. This improvement in the ultrastructure of lung by the phytochemicals may have led to decreased lung weights by reducing the levels of pro-inflammatory enzyme COX-2 that in turn also assisted in reducing the tumor incidence as well as multiplicity (14).

Therefore, curcumin and quercetin show great prospects in dealing with the condition of lung carcinogenesis and greater improvement was observed in the combined treatment group more frequently. The results of the present study suggest these phytochemicals hold great potential to be used as an effective preventive measure against the occurrence of lung cancer in a section of human population with a family history of lung cancer, as well those who are constantly exposed to carcinogens from different sources.

In conclusion, the present findings show that a combination approach in the supplementation of phytochemicals can effectively produce ultrastructural changes at the transmission electron microscopic level during lung carcinogenesis.

References

1. He Z, Xia Y, Tang S, Chen Y and Chen L: Detection of occult tumor cells in regional lymph nodes is associated with poor survival in pN0 non-small cell lung cancer: A meta-analysis. *J Thorac Dis* 8: 375-385, 2016.

2. Ferlay J, Shin HR, Bray F, Forman D, Mathers C and Parkin DM: Estimates of worldwide burden of cancer in 2008: GLOBOCAN 2008. *Int J Cancer* 127: 2893-2917, 2010.
3. Yamamoto S, Huang D, Du L, Korn RL, Jamshidi N, Burnette BL and Kuo MD: Radiogenomic analysis demonstrates associations between 18F-fluoro-2-deoxyglucose PET, prognosis, and epithelial-mesenchymal transition in non-small cell lung cancer. *Radiology*: Apr 15, 2016 (Epub ahead of print).
4. Orfali G, Duarte AC, Bonadio V, Martinez NP, de Araújo ME, Priviero FB, Carvalho PO and Priolli DG: Review of anticancer mechanisms of isoquercetin. *World J Clin Oncol* 7: 189-199, 2016.
5. Malhotra A, Nair P and Dhawan DK: Study to evaluate molecular mechanisms behind synergistic chemo-preventive effects of curcumin and resveratrol during lung carcinogenesis. *PLoS One* 9: e93820, 2014.
6. Sun N, Sun P, Lv H, Sun Y, Guo J, Wang Z, Luo T, Wang S and Li H: Matrine displayed antiviral activity in porcine alveolar macrophages co-infected by porcine reproductive and respiratory syndrome virus and porcine circovirus type 2. *Sci Rep* 6: 24401, 2016.
7. Morales AG, Stempinski ES, Xiao X, Patel A, Panna A, Olivier KN, McShane PJ, Robinson C, George AJ, Donahue DR, *et al*: Micro-CT scouting for transmission electron microscopy of human tissue specimens. *J Microsc*: Feb 8, 2016 (Epub ahead of print).
8. Flodby P, Kim YH, Beard LL, Gao D, Ji Y, Kage H, Liebler JM, Minoo P, Kim KJ, Borok Z and Crandall ED: Knockout mice reveal a major role for alveolar epithelial type I cells in alveolar fluid clearance. *Am J Respir Cell Mol Biol*: Apr 11, 2016 (Epub ahead of print).
9. El-Zein RA, Lopez MS, D'Amelio AM Jr, Liu M, Munden RF, Christiani D, Su L, Tejera-Alvarez P, Zhai R, Spitz MR, *et al*: The cytokinesis-blocked micronucleus assay as a strong predictor of lung cancer: Extension of a lung cancer risk prediction model. *Cancer Epidemiol Biomarkers Prev* 23: 2462-2470, 2014.
10. Bantikassegn A, Song X and Politi K: Isolation of epithelial, endothelial, and immune cells from lungs of transgenic mice with oncogene-induced lung adenocarcinomas. *Am J Respir Cell Mol Biol* 52: 409-417, 2015.
11. Ahn H, Lee K, Kim JM, Kwon SH, Lee SH, Lee SY and Jeong D: accelerated lactate dehydrogenase activity potentiates osteoclastogenesis via NFATc1 signaling. *PLoS One* 11: e0153886, 2016.
12. Crystal RG: Airway basal cells. The 'smoking gun' of chronic obstructive pulmonary disease. *Am J Respir Crit Care Med* 190: 1355-1362, 2014.
13. Bhatia A and Kumar Y: Cancer cell micronucleus: an update on clinical and diagnostic applications. *APMIS* 121: 569-581, 2013.
14. Said-Elbahr R, Nasr M, Alhnan MA, Taha I and Sammour O: Nebulizable colloidal nanoparticles co-encapsulating a COX-2 inhibitor and a herbal compound for treatment of lung cancer. *Eur J Pharm Biopharm* 103: 1-12, 2016.